I&EC research
Industrial & Engineering Chemistry Research

Article

pubs.acs.org/IECR

Effect of Phosphate Salts (Na_3PO_4, Na_2HPO_4, and NaH_2PO_4) on Ag_3PO_4 Morphology for Photocatalytic Dye Degradation under Visible Light and Toxicity of the Degraded Dye Products

Pongsaton Amornpitoksuk,*[,†,§] Khanitta Intarasuwan,[†] Sumetha Suwanboon,[‡,§] and Jonas Baltrusaitis[⊥]

[†]Department of Chemistry and Center of Excellence for Innovation in Chemistry, Faculty of Science, Prince of Songkla University, Hat-Yai, Songkhla 90112, Thailand

[‡]Department of Materials Science and Technology, Faculty of Science, Prince of Songkla University, Hat-Yai, Songkhla 90112, Thailand

[§]Center of Excellence in Nanotechnology for Energy (CENE), Prince of Songkla University, Hat-Yai, Songkhla 90112, Thailand

[⊥]PhotoCatalytic Synthesis Group, Faculty of Science and Technology, MESA+ Institute, University of Twente, Meander 229, P.O. Box 217, 7500 AE Enschede, The Netherlands

Supporting Information

ABSTRACT: Ag_3PO_4 was synthesized by the precipitation method using three different types of phosphate salts (Na_3PO_4, Na_2HPO_4, and NaH_2PO_4) as a precipitating agent. Hydrolysis of each phosphate salt gave a specific pH that affected the purity and morphology of the prepared Ag_3PO_4. The Ag_3PO_4 prepared from Na_2HPO_4 showed the best photocatalytic activity induced by visible light to degrade methylene blue dye. During the photocatalytic process, Ag_3PO_4 decomposed and produced metallic Ag, and this evidence was confirmed by the X-ray diffraction technique and X-ray photoelectron spectroscopy. The photocatalytic efficiency decreased with the number of recycles used. This Ag_3PO_4 photocatalyst also degraded another cationic dye, rhodamine B, but did not degrade reactive orange, an anionic dye. The degraded products produced by the photocatalysis had lower toxicities than the untreated dyes using *Chlorella vulgaris* as a bioindicator.

1. INTRODUCTION

The wastewater containing dye wastes from the textile industry has many effects on humans, animals, and the ecosystem because many dyes are very toxic to aquatic life and the human body.[1] It can also inhibit the photosynthesis of submerged plants, as dyes are highly colored waste that can reduce the penetration of the light.[2] The treatment of this waste by an advanced oxidation process using photocatalysts is one of the most effective methods used because of its high efficiency, the possibilities for recycling, and the energy reduction (can use sunlight) and because it is environmentally friendly.[3] Although metal-oxide-based photocatalysts such as TiO_2 and ZnO have been widely used for the photocatalytic degradation of dyes, these photocatalysts have a wide energy band gap, so they effectively use only light in the UV region.[4,5] In sunlight, the UV rays are only a small portion compared to the visible light, so the development of visible-light-based photocatalysts has recently become a hot issue.[6]

In recent years, silver phosphate (Ag_3PO_4) is a new type of photocatalyst that is highly effective in visible light.[7−11] Yi et al.[7] reported that Ag_3PO_4 has a direct band gap of about 2.43 eV that can absorb energy with a wavelength shorter than about 530 nm. The dominant active species in the photocatalytic degradation process using Ag_3PO_4 as photocatalyst has been reported to produce photoinduced holes.[8] Ag_3PO_4 can be synthesized by several methods but the precipitation or ion-exchange methods usually have been of interest because it is a simple method and a low-cost technique. Na_2HPO_4 is the most popular precipitating agent to form Ag_3PO_4 powders;[9,10] however, some different phosphate sources such as Na_3PO_4 have been reported for use.[7,9] However, the effect of different types of precipitating agents on the morphology of Ag_3PO_4 has not been reported. It appears that the type of precipitating agent can control the morphology of Ag_3PO_4 and this, therefore, has an effect on its properties, including its photocatalytic activity.

In this work, we report the effect of phosphate salts (Na_3PO_4, Na_2HPO_4, and NaH_2PO_4) on the structure, morphology, and photocatalytic activity of Ag_3PO_4 prepared through a precipitation method. As there have been no reports on the potential toxicity of dyes after photocatalytic degradation using Ag_3PO_4 as photocatalyst, this treated solution was also used in a preliminary test to inhibit the growth of the *Chlorella vulgaris* used as a bioindicator.

2. EXPERIMENTAL SECTION

2.1. Synthesis. Silver phosphate (Ag_3PO_4) was prepared by the precipitation method. In a typical procedure, 0.005 mol of the phosphate salt (Na_3PO_4, Na_2HPO_4, and NaH_2PO_4) was dissolved in 100 mL of distilled water. This solution was added dropwise to a 0.1 M $AgNO_3$ solution prepared by dissolving 0.01 mol $AgNO_3$ in 100 mL of distilled water. The yellow suspension was heated at 80 °C for 1 h under continuous

Received: June 10, 2013
Revised: October 10, 2013
Accepted: November 18, 2013
Published: November 18, 2013

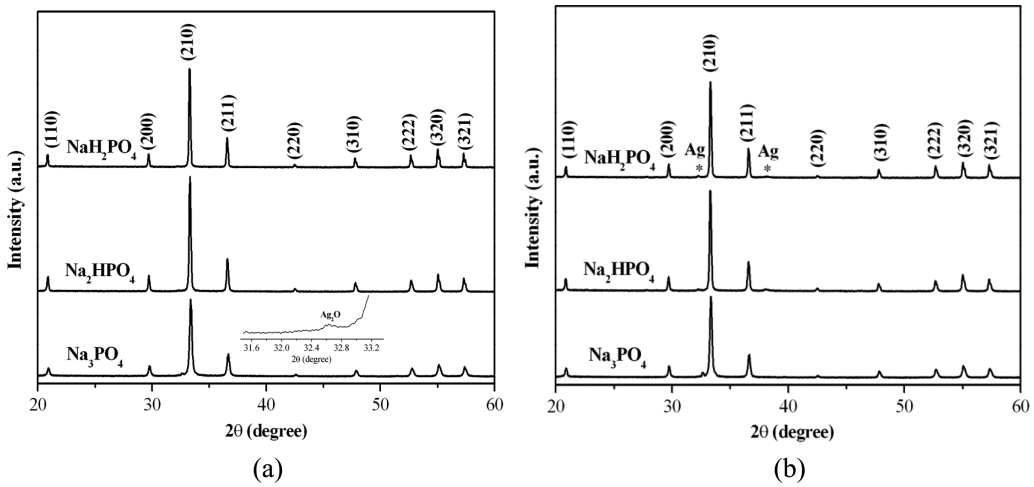

Figure 1. X-ray diffraction patterns of Ag_3PO_4 prepared from three different types of phosphate salts as a precipitating agent (a) before and (b) after photocatalysis.

stirred conditions and then filtered, rinsed with distilled water 3 times, dried overnight, and heated at 100 °C for 1 h. Ag_3PO_4 prepared from Na_3PO_4, Na_2HPO_4, and NaH_2PO_4 have been labeled "Ag_3PO_4 (H-0)", "Ag_3PO_4 (H-1)" and "Ag_3PO_4 (H-2)", respectively.

2.2. Characterization. The structural identification and morphology of the Ag_3PO_4 powders were carried out using an X-ray diffractometer (XRD, X'Pert MPD, Philips) with Cu Kα radiation at a wavelength of 0.15406 nm and a scanning electron microscope (SEM, QUANTA 400, FEI), respectively. The oxidation states of Ag in Ag_3PO_4 powders were analyzed by X-ray photoelectron spectroscopy (Quantera SXM, Physical Electronics) using Al Kα monochromatic radiation at 1486.6 eV. All binding energies were also calibrated to the C 1s peak at 284.8 eV.

2.3. Photocatalytic Study. The photocatalytic activity of the prepared Ag_3PO_4 powders was investigated by decolorization of methylene blue (MB), rhodamine B (RhB), and reactive orange (RO) used as the dry stuff pollutant under a TL-D/35 fluorescent tube (18W, Philips) that were claimed to have no UV emission from the data sheet. In this work, 0.15 g of the Ag_3PO_4 powder was added to a 1×10^{-5} M dye aqueous solution and first stirred in dark conditions to study the sorption−desorption equilibrium phenomena. After that, this suspension was irradiated under 3 parallel fluorescent tubes and 3 mL of dye solution was sampled after each 10 min of irradiation. The remaining dye concentration after the required irradiation was determined by the absorption techniques using a UV−vis spectrophotometer (Lambda 25, Perkin-Elmer).

2.4. Toxicity Test. The ecotoxicity tests were carried out using the freshwater unicellular green algae *Chlorella vulgaris*. The stock of *Chlorella vulgaris* was cultured in a nutrient medium described by Athibai.[12] All nutrient media and equipment were sterilized to ensure that there were no contaminating microorganisms. The 100 mL of stock algal cells were propagated in a 500 mL glass bottle containing 300 mL of liquid nutrient medium and kept at 25 ± 2 °C under cool white fluorescent lighting (18 W) with a 12 h light and 12 h dark light photoperiod. Agitation was performed by bubbling with filtered air.

The inoculum of *Chlorella vulgaris* provided a concentration of around 2×10^6 cell/mL in each flask that contained 4 mL of MB or RhB solution before and after the photocatalytic process. Inoculated nutrient medium (0.5 mL) was added into each flask and then incubated at 25 ± 2 °C while being continuously shaken (100 rpm). Illumination was provided by white fluorescent light (18 W) following a day/night period of 12 h/12 h for 72 h. To evaluate the cell density, 100 μL of the testing solution containing the *Chlorella vulgaris* was pipetted into formaldehyde to stop cell division and 10 μL of the resulting solution was pipetted onto a hemacytometer slide, and the number of cells was evaluated using an optical microscope. The data represent the mean ± standard deviation of triplicate measurements from each treatment.

3. RESULTS AND DISCUSSION

3.1. Structure and Morphology. The X-ray diffraction (XRD) patterns of Ag_3PO_4 prepared with three different types of phosphate salts, as precipitating agents, are shown in Figure 1a, and their lattice parameters, *a*, resolved by Rietveld method are also presented in Table 1. The Ag_3PO_4 (H-1) and Ag_3PO_4 (H-2) are clearly crystallized in the cubic structure as all diffraction peaks of these samples are well matched with JCPDS card number 06-0505. In contrast, the XRD pattern of the Ag_3PO_4 (H-0) showed a mixed phase between Ag_3PO_4 and Ag_2O (JCPDS card number 41-1104) as shown in Figure 1a. This evidence does not agree with the results reported by Wang et al.[9] This could be due to a higher amount of Na_3PO_4 being used in this work compared with that used by Wang et al.,[9] and this would affect the pH of the solution. From the basic chemistry, Na_3PO_4 is a basic salt that can dissolve in water and produces OH^- species. In this work, the pH of this solution is

Table 1. pH Values of the Precipitating Agent and the Lattice Parameters, Crystallite Sizes, Band Gaps, and BET Surface Areas of the Ag_3PO_4 Powders Prepared from Three Different Types of Phosphate Salts

precipitating agent	initial pH	lattice parameter, *a* (Å)	crystallite size (nm)	band gap (eV)	BET (m^2/g)
Na_3PO_4	12.10	6.0009(2)	49.15		8.08
Na_2HPO_4	9.50	6.0132(1)	54.14	2.42	4.02
NaH_2PO_4	4.94	6.0151(4)	60.15	2.41	0[a]

[a]Approaches zero.

equal to 12.10, at which point Ag^+ can react with OH^- to form AgOH and then decompose spontaneously to Ag_2O before heating. This resulted in a change of the suspension's color from yellow to brown. Both the Na_2HPO_4 and Na_3PO_4 are basic salts that produce the OH^- after hydrolysis, but there is no sign of the Ag_2O phase in the XRD pattern of Ag_3PO_4 prepared from Na_2HPO_4. This result comes from the effect of the pH on the formation of Ag_2O, and this hypothesis was subjected to a preliminary test by the addition of Ag^+ to alkaline solutions at various pH values. The brown precipitants (Figure 2) were clearly observed at a pH > 10; however, a very slight

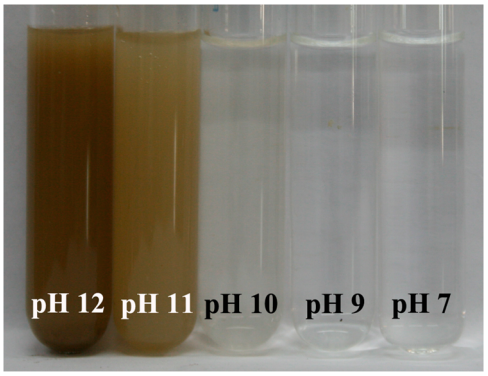

Figure 2. Photograph of the results from the mixing between Ag^+ in OH^- solution at different pHs and D.I. water.

brown solid was observed at pH 10 (difficult to see). The starting solutions of 0.01 mol Na_2HPO_4 (basic salt) and NaH_2PO_4 (acidic salt) in 100 mL of distilled water have pH values equal to 9.50 and 4.94, respectively. For the Na_2HPO_4, the pH of its solution was less than 10, and this is one reason why the Ag_2O phase did not appear in the XRD pattern. On the other hand, NaH_2PO_4 is an acidic salt that does not produce any OH^- species, so the Ag_2O cannot be detected in the XRD pattern. Although Na_2HPO_4 and Na_3PO_4 are the basic salts that generate OH^- species, the major product from reactions between Ag^+ and their basic salts is Ag_3PO_4 (not AgOH) because the K_{sp} of Ag_3PO_4 (1.8×10^{-18}) is less than the K_{sp} of AgOH (2×10^{-8}).

Figure 1b shows the XRD patterns of all Ag_3PO_4 prepared from the three different types of precipitating agents after photocatalysis. All the prepared Ag_3PO_4 compounds clearly show an additional peak at $2\theta = 37.6°$, which usually has been reported to be a diffraction peak of metallic silver (JCPDS card number 04-0738),[8,9] and the color of the Ag_3PO_4 after photocatalysis changed to yellow-black. This comes from the reaction between the holes at the valence band of Ag_3PO_4 and the dyes; thus, Ag_3PO_4 can decompose to Ag(0) and PO_4^{3-}, as previously established.[8,9]

The morphologies of Ag_3PO_4 prepared with the different types of precipitating agents are shown in Figure 3. The particle size relates to their crystallite size calculated by the Schrrer equation (Table 1). The surface areas of Ag_3PO_4 prepared using Na_3PO_4, Na_2HPO_4, and NaH_2PO_4 as precipitating agents are 8.08, 4.02, and 0 m^2/g, respectively.

From an ionic reaction, the Ag^+ ion reacts with PO_4^{3-} ion to form Ag_3PO_4(s). When anisotropic growth is considered, the Ag_3PO_4 shows a rhombic dodecahedral morphology as the growth rate of the different crystallographic planes are in the order of $V_{\{110\}} > V_{\{100\}} > V_{\{111\}}$.[13] In Na_3PO_4, the Ag_2O, as an impurity, acts like an obstacle that inhibits the grain growth, and this phenomenon is known as Zener pinning.[14] The limiting grain diameter (D) is generally a function of the mean radius (r) and the volume faction (F_v) of the pinning particles as follows:[14]

$$D = (4\alpha r)/(3F_v) \quad (1)$$

where α is a geometrical constant. The presence of Ag_2O provides a secondary phase that could retard the particle growth; therefore, the particle size of Ag_3PO_4 prepared from Na_3PO_4 is the smallest. The pinning particles should surround the Ag_3PO_4 nuclei during the growth process, and this produces a small spherical-like shape. For Na_2HPO_4, although Ag_2O is not detectable in this system, the OH^- generated from the hydrolysis of HPO_4^- could interact with Ag^+ to form AgOH, and it is possible that very small amounts of AgOH would decompose to Ag_2O. This will produce a small Zener drag, so the Ag_3PO_4 is then an irregular shape. According to eq 1, the particle sizes of Ag_3PO_4 prepared from Na_2HPO_4 are bigger than those prepared from Na_3PO_4. Another possible way should come from the competition between the OH^- and PO_4^{3-} that reacts with Ag on the surface of the Ag_3PO_4 nuclei during the growth process. In the NaH_2PO_4 solution, there is neither OH^- nor Ag_2O species in the system, so the growth of the Ag_3PO_4 is anisotropic growth and produces the biggest particles in a rhombic dodecahedral-like shape.

3.2. Oxidation State. The oxidation states of all prepared Ag_3PO_4 before and after photocatalysis were investigated by the X-ray photoelectron spectroscopy (XPS) technique. As presented in Figure 4a, the Ag 3d spectra of as-prepared Ag_3PO_4 powders are composed of two characteristic peaks around 373.7 and 367.7 eV. These can be attributed to the Ag $3d_{3/2}$ and Ag $3d_{5/3}$ binding energies, respectively.[15,16] As the peak width at half-maximum intensity of Ag $3d_{5/2}$ of Ag_3PO_4 (H-0) is more than those values of Ag_3PO_4 (H-1) and Ag_3PO_4 (H-2) and its XRD pattern shows the secondary phase as shown in Figure 1a, this peak is therefore fitted by the nonlinear

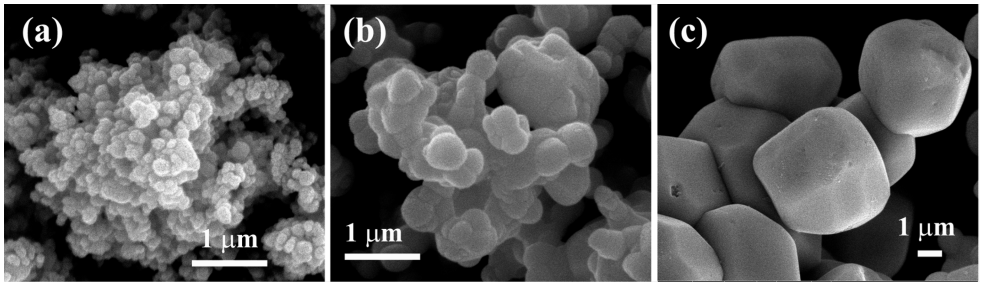

Figure 3. Scanning electron microscope images of Ag_3PO_4 prepared from (a) Na_3PO_4, (b) Na_2HPO_4, and (c) NaH_2PO_4.

dx.doi.org/10.1021/ie401821w | Ind. Eng. Chem. Res. 2013, 52, 17369−17375

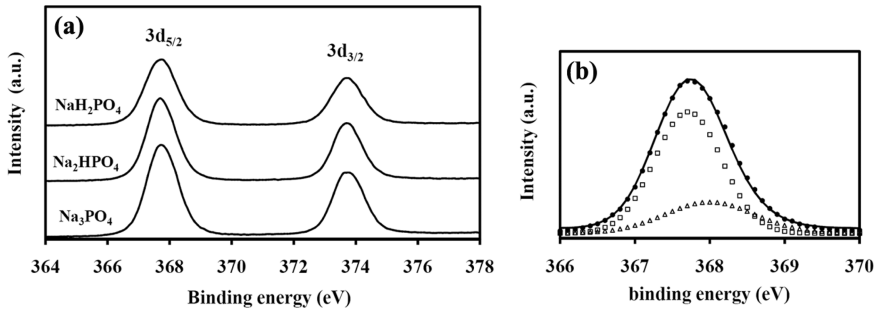

Figure 4. X-ray spectroscopy spectra of (a) Ag 3d for as-prepared Ag_3PO_4 powders using three different types of precipitating agents and (b) the deconvolution for Ag $3d_{5/2}$ peak for Ag_3PO_4 prepared from Na_3PO_4.

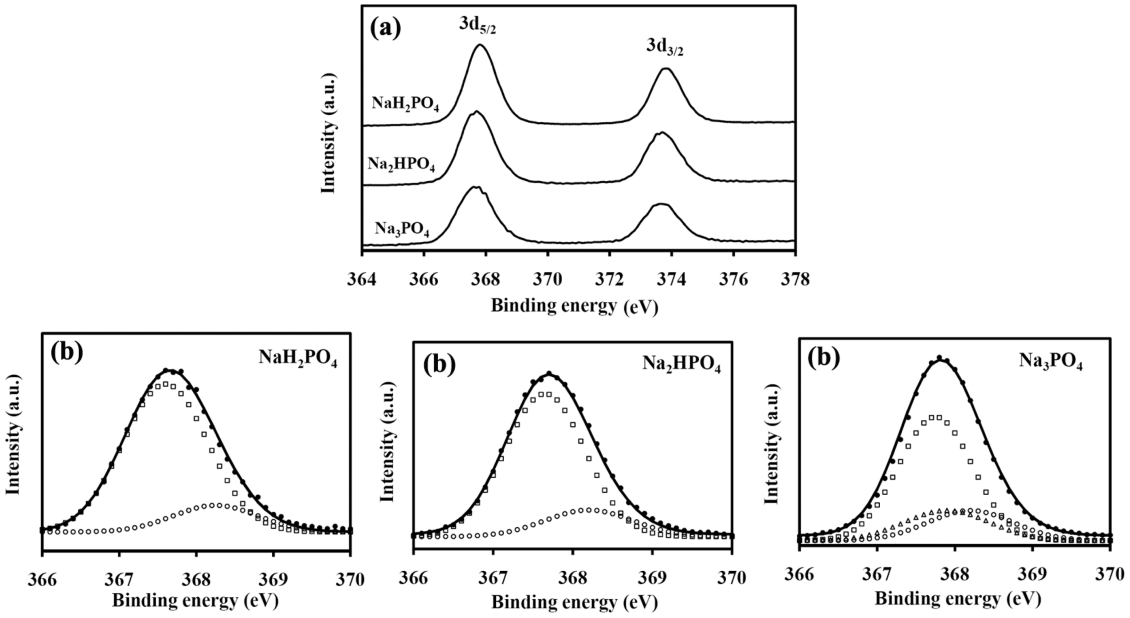

Figure 5. X-ray spectroscopy spectra of (a) Ag 3d for Ag_3PO_4 powders using three different types of precipitating agents after photocatalysis and (b) the deconvolution for their Ag $3d_{5/2}$ peaks.

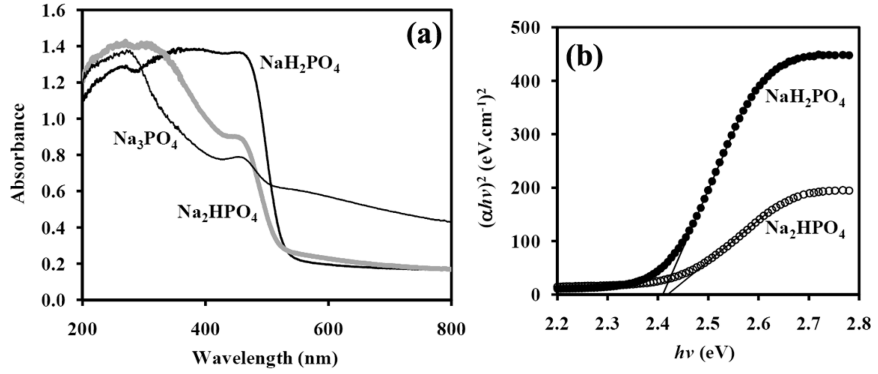

Figure 6. Absorption spectra (a) and a plot of $(\alpha h\nu)^2$ vs. $h\nu$ (b) of Ag_3PO_4 prepared from three different types of precipitating agents.

least-squares fit program using a Gaussian function. From deconvolution, as shown in Figure 4b, an additional peak at 367.9 eV was assigned to the binding energy of Ag $3d_{5/2}$ of Ag_2O,[17] and this was in agreement with the XRD result. After photocatalysis, all Ag_3PO_4 powders show the spectra of Ag 3d, as presented in Figure 5. Compared to the as-prepared Ag_3PO_4 (before photocatalysis) (Figure 4), the additional binding energy at 368.2 eV is attributed to metallic Ag (Figure 5b). This comes from the decomposition of Ag_3PO_4 during photocatalysis, as mentioned in section 3.1.

3.3. Optical Properties. The UV−vis spectra of Ag_3PO_4 prepared with three different types of precipitating agents are presented in Figure 6a. The shoulder around 467 nm for all samples indicated the electron transition from a valence band to a conduction band, whereas the broad band higher than 500 nm comes from the absorption of Ag_2O (brown-black color).

dx.doi.org/10.1021/ie401821w | Ind. Eng. Chem. Res. 2013, 52, 17369−17375

The band gap energy of a semiconductor including Ag_3PO_4 is usually calculated by the following equation:[18]

$$\alpha h\nu = A(h\nu - E_g)^{n/2}$$

where α is the absorption coefficient, h is the Planck constant, ν is the light frequency, E_g is the band gap energy, and A is a constant. When it was made into an extrapolation form of the linear part of a plot of $(\alpha h\nu)^2$ versus $h\nu$, the $h\nu$ axis intercept was the direct band gap value. Their values for Ag_3PO_4 (H-2) and Ag_3PO_4 (H-1) were equal to 2.41 and 2.42, respectively, (Figure 6b). From the relationship between the band gap energy and particle size (Table 1), it is generally observed that the reduction in particle size leads to an increase of the band gap energy. However, the direct band gap for Ag_3PO_4 (H-0) was not estimated because of the overlap of the absorption spectra between Ag_3PO_4 and Ag_2O.

3.4. Photocatalytic Study. Figure 7 shows the variations of the photocatalytic degradation of MB as a function of

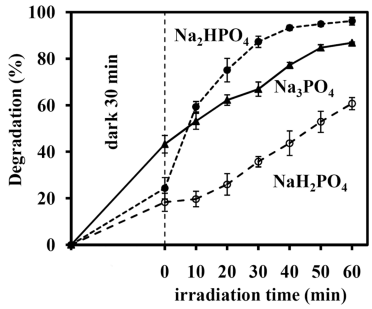

Figure 7. Photocatalytic degradation of MB by Ag_3PO_4 prepared from three different types of precipitating agents under visible light irradiation and in the dark condition.

irradiation times. The adsorption in the dark condition can clearly decrease the MB concentration, but this is negligible compared to its reduction by a photocatalytic process. The adsorption ability corresponded to both their particle size and their surface area (see section 3.1.) After irradiation, the photocatalytic decolorization efficiencies increased in the order: Ag_3PO_4 (H-1) > Ag_3PO_4 (H-0) > Ag_3PO_4 (H-2) (Figure 7). The Ag_3PO_4 (H-2) crystallized in large particle sizes, which has a low surface area, so its photocatalytic activity is very low. Although Ag_3PO_4 (H-0) has the most surface area compared to those of the prepared Ag_3PO_4, the coexistence of the secondary phase as Ag_2O could also reduce its active surface area, and this then leads to a decrease of its photocatalytic activity.

The recycling experiments of Ag_3PO_4 prepared with the three different types of precipitating agents after photocatalysis for 1 h are presented in Figure 8. The efficiencies of all Ag_3PO_4 decreased with the number of uses because of an increment to the Ag phase during photocatalysis.[9] For comparison with all samples, Ag_3PO_4 (H-1) showed a good recycling ability, as seen in Figure 8. For the first use, the photocatalytic decolorization of Ag_3PO_4 (H-0) was better than the activity of Ag_3PO_4 (H-2). Although their efficiencies decreased continuously with the recycling number, in the third recycle, the photocatalytic activity of Ag_3PO_4 (H-2) was better than that of Ag_3PO_4 (H-0).

Not only methylene blue (MB) but also other dyes such as rhodamin B (RhB, as a cationic dye) and reactive orange (RO, as an anionic dye) were also selected to study the photocatalytic activity of Ag_3PO_4 (H-1). Figure 9 shows the

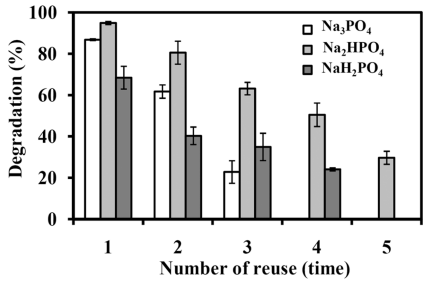

Figure 8. Dependence of the photocatalytic degradation of MB by Ag_3PO_4 prepared from three different types of precipitating agents after 1 h of irradiation with the number of reuses.

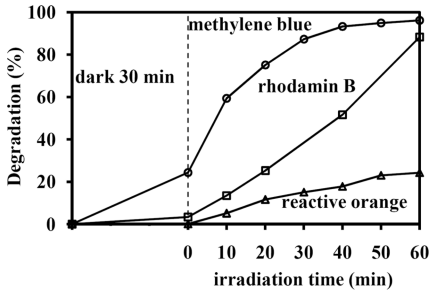

Figure 9. Photocatalytic efficiencies of different dyes by Ag_3PO_4 prepared from Na_2HPO_4 using irradiation with visible light and in the dark condition.

photocatalytic efficiency of Ag_3PO_4 (H-1) for degrading the three dyes. For the cationic dye, Ag_3PO_4 (H-1) can degrade MB better than RhB because it probably comes from the large and more complicated structures of the RhB dye. For the RO used as an anionic dye, it showed only a small reduction of the RO concentration over 1 h of irradiation, and this evidence could also apply to other anionic dyes such as methyl orange.[8] This evidence can be explained by the interaction between the charge on the surface of Ag_3PO_4 and the charge of dye molecules. The pH on the point of zero change (pHpzc) of Ag_3PO_4 (H-1) was investigated by a pH drift method and its determination followed the same procedure as that reported by Wibowo et al.[19] The results as presented in Supporting Information Figure S1, show a pHpzc ~6.65. Therefore, the surface of Ag_3PO_4 has a negative charge in neutral solution, and this repulses the anionic dyes. This could be confirmed by the adsorption of dyes in the dark. Returning to Figure 9, the Ag_3PO_4 (H-1) can clearly adsorb cationic dyes better than reactive orange (including methyl orange but the data is not shown). In RO, the Ag_3PO_4 (H-1) after irradiation still has a yellow color, whereas the Ag_3PO_4 (H-1) changes to a yellow-black color after photocatalyis in the MB and RhB solutions.

For the Ag_3PO_4, several research groups[7−11] have reported that both ·OH and $\cdot O_2^-$ species are not the main reactive species in this photocatalytic process, but the reactivity comes from the interaction between the photoinduced holes with the pollutant molecules. The direct hole oxidation can degrade not only dye molecules but also phenolic compounds such as bisphenol A, as presented in Supporting Information Figure S2, and that is in agreement with the results reported by Katsumata et al.[20]

3.5. Toxicity of the Treated Dye Solution. A preliminary toxicity test of the treated dye solution was studied using the inhibition of growth of *Chlorella vulgaris* as an ecological indicator. Although there are many ecological indicators, such

dx.doi.org/10.1021/ie401821w | Ind. Eng. Chem. Res. 2013, 52, 17369−17375

as fish, crustacean, bacteria, algae, and so on, a green algae such as *Chlorella sp.*, are often more sensitive to contaminants or chemicals than the others in the same aquatic environments.[21] Because Ag_3PO_4 does not degrade RO well, the toxicity to *C. vulgaris* cells was investigated only in the solution of the MB and RhB after 100 min of irradiation. Figure 10 shows the

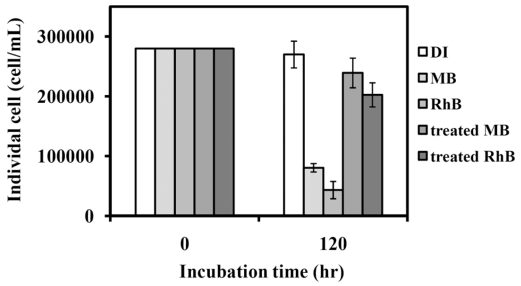

Figure 10. Individual cells of *Chlorella vulgaris* in a 1×10^{-5} M MB and RhB solutions before and after photocatalysis.

density of individual cells (cell/mL) for *C. vulgaris* in 1×10^{-5} M MB and RhB solutions before and after photocatalysis. For MB and RhB, the number of individual cells in the dyes solutions treated with Ag_3PO_4 (H-1) were higher than those in the initial dye solutions. We can assume 2 possible scenarios: (1) the degraded products from photocatalysis have low toxicity to *Chlorella vulgaris* cells or (2) if the degraded products were toxic, the concentration of these species was too low to effectively inhibit the growth of *C. vulgaris*.

4. CONCLUSIONS

The type of phosphate salt used as a precipitating agent can affect the purity, morphology, particle size, and photocatalytic activity of the prepared Ag_3PO_4 powder. Using Na_3PO_4, Ag^+ can react with OH^- to form Ag_2O that is coprecipitated with Ag_3PO_4. When the precipitating agents are NaH_2PO_4 and Na_2HPO_4, the products showed only the pure phase of Ag_3PO_4 because the pH of the solution was less than 10. Ag_3PO_4 prepared from Na_2HPO_4 showed better photocatalytic efficiency compared to those prepared from NaH_2PO_4 and Na_3PO_4. This photocatalyst can degrade methylene blue and rhodamine B but did not effectively degrade reactive orange as a model for an anionic dye because of the repulsive force between the negative charges on the surface of the Ag_3PO_4 and dye. The treated methylene blue and rhodamine B solutions have low toxicity against *Chlorella vulgaris* cells compared with that of the untreated dyes.

■ ASSOCIATED CONTENT

Supporting Information

Determination of the point of zero change using a pH drift method; the changes of the absorption spectra of bisphenol A over Ag_3PO_4 at different irradiation times. This material is available free of charge via the Internet at http://pubs.acs.org.

■ AUTHOR INFORMATION

Corresponding Author

*P. Amornpitoksuk. E-mail: ampongsa@yahoo.com. Phone: 00 66 74288438. Fax: 00 66 74558841.

Notes

The authors declare no competing financial interest.

■ ACKNOWLEDGMENTS

This research was supported by Prince of Songkla University under contact number SCI560329S. The author acknowledges the Center of Excellence for Innovation in Chemistry (PERCH-CIC), Office of the Higher Education Commission, Ministry of Education. We would also like to thank Dr. Brian Hodgson for assistance with the English.

■ REFERENCES

(1) Chen, K. C.; Wua, J. Y.; Huang, C. C.; Liang, Y. M.; Hwang, S. C. J. Decolorization of azo dye using PVA-immobilized microorganisms. *J. Biotechnol.* **2003**, *101*, 241−252.

(2) Solís, M.; Solís, A.; Perez, H. I.; Manjarrez, N.; Flores, M. Microbial decolouration of azo dyes: A review. *Process Biochem.* **2012**, *47*, 1723−1748.

(3) Fujishima, A.; Zhang, X.; Tryk, D. A. Heterogeneous photocatalysis: Fromwater photolysis to applications in environmental cleanup. *Int. J. Hydrogen Energy* **2007**, *32*, 2664−2672.

(4) Paz, Y. Application of TiO_2 photocatalysis for air treatment: Patents' overview. *Appl. Catal., B* **2010**, *99*, 448−460.

(5) Liqiang, J.; Xiaojun, S.; Jing, S.; Weimin, C.; Zili, X.; Yaoguo, D.; Honggang, F. Review of surface photovoltage spectra of nanosized semiconductor and its applications in heterogeneous photocatalysis. *Sol. Energy Mater. Sol. Cells* **2003**, *79*, 133−151.

(6) Malato, S.; Fernández-Ibáñez, P.; Maldonado, M. I.; Blanco, J.; Gernjak, W. Decontamination and disinfection of water by solar photocatalysis: Recent overview and trends. *Catal. Today* **2009**, *147*, 1−59.

(7) Yi, Z.; Ye, J.; Kikugawa, N.; Kako, T.; Ouyang, S.; Stuart-Willams, H.; Yang, H.; Cao, J.; Luo, W.; Li, Z.; Liu, Y.; Withers, R. L. An orthophosphate semiconductor with photooxidation properties under visible light irradiation. *Nat. Mater.* **2010**, *9*, 559−564.

(8) Gem, M.; Zhum, N.; Zho, Y.; Li, J.; Liu, L. Sunlight-assisted degradation of dye pollutant in Ag_3PO_4 suspension. *Ind. Eng. Chem. Res.* **2012**, *51*, 5167−5173.

(9) Wang, H.; Bai, Y.; Yang, J.; Lang, X.; Li, J.; Guo, L. A Facile way to rejuvenate Ag_3PO_4 as a recyclable highly efficient photocatalyst. *Chem.—Eur. J.* **2012**, *18*, 5524−5529.

(10) Khan, A.; Qamart, M.; Muneer, M. Synthesis of highly active visible-light-driven colloidal silver orthophosphate. *Chem. Phys. Lett.* **2012**, *519*−*520*, 54−58.

(11) Vu, T. A.; Dao, C. D.; Hoang, T. T. T.; Nguyen, K. T.; Le, G. H.; Dang, P. T.; Tran, H. T. K.; Nguyen, T. V. Highly photocatalytic activity of novel nano-sized Ag_3PO_4 for Rhodamine B degradation under visible light irradiation. *Mater. Lett.* **2013**, *92*, 57−60.

(12) Athibai, S. Species diversity and distribution of the family Brachionidae (Rotifers) in Thailand. *Ph.D. Thesis*, Khon Kaen University, 2008.

(13) Bate, P. The effect of deformation on grain growth in zener pinning systems. *Acta Mater.* **2001**, *49*, 1453−1461.

(14) Bi, Y.; Ouyang, S.; Cao, J.; Ye, J. Facial synthesis of rhombic dodecahedral AgX/Ag_3PO_4 (X = Cl, Br, I) heterocrystals with enhanced photocatalytic properties and stabilities. *Phys. Chem. Chem. Phys.* **2011**, *13*, 10071−10075.

(15) Teng, W.; Li, X.; Zhao, Q.; Zhao, J.; Zhang, D. In situ capture of active species and oxidation mechanism of RhB and MB dyes over sunlight-driven Ag/Ag_3PO_4 plasmonic nanocatalyst. *Appl. Catal., B* **2012**, *125*, 538−545.

(16) Liu, Y.; Fang, L.; Lu, H.; Li, Y.; Hu, C.; Yu, H. One-pot pyridine-assisted synthesis of visible-light-driven photocatalyst Ag/Ag_3PO_4. *Appl. Catal., B* **2012**, *115*−*116*, 245−252.

(17) Waterhouse, G. I. N.; Bowmaker, G. A.; Metson, J. B. Oxidation of a polycrystalline silver foil by reaction with ozone. *Appl. Surf. Sci.* **2001**, *183*, 191−204.

(18) Yu, J.; Li, C.; Liu, S. Effect of PSS on morphology and optical properties of ZnO. *J. Colloid Interface Sci.* **2008**, *326*, 433−438.

(19) Wibowo, N.; Setiyadhi, L.; Wibowo, D.; Setiawan, J.; Ismadji, S. Adsorption of benzene and toluene from aqueous solution onto

activated carbon and its acid and heat treated forms: Influence of surface chemistry on adsorption. *J. Hazard. Mater.* **2007**, *146*, 237−42.
(20) Katsumata, H.; Taniguchi, M.; Kaneco, S.; Suzuki, T. Photocatalytic degradation of bisphenol A by Ag_3PO_4 under visible light. *Catal. Comm.* **2013**, *34*, 30−34.
(21) Wong, S. L. Algal assay approaches to pollution studied in aquatic system. In *Pollution and Biomonitoring*; Rana, B. C., Ed.; Tata McGraw-Hill Publishing Company Ltd.: New Delhi, 1995; pp 26−51.

■ NOTE ADDED AFTER ASAP PUBLICATION

This paper was published ASAP on November 22, 2013, with an error in Figure 1b. The figure was corrected and the paper was reposted on November 26, 2013.